AutoMatic integration of electrocardiogram and cardiac Magnetic Resonance Imaging to guide caTheter-based substrate ablation for Ventricular Arrhythmias – The MERIT-VA Project

Beatriz Jáuregui, MD[a*]; Guillermo Jimenez-Perez[b*]; David Soto-Iglesias, PhD[a]; Diego Penela, MD, PhD[a]; Ramón Trueba[c]; Xavier Planes[c]; Luis Serra[c]; Oscar Camara[b]; Antonio Berruezo, MD, PhD[a]

[a]*Heart Institute, Teknon Medical Center, Barcelona, Spain;* [b]*PhySense Group, BCN-MedTech Unit, Department of Information and Communication Technologies, Universitat Pompeu Fabra, Barcelona, Spain;* [c]*ADAS 3D Medical SL, Barcelona, Spain*

**Both authors equally contributed to this work.*

Conflict of interest: Dr. Berruezo and Luis Serra are stockholders of ADAS 3D Medical SL. David Soto-Iglesias is an employee of Biosense Webster Inc. The other authors have no other relevant affiliations or financial involvement with any organization or entity with a financial interest in or financial conflict with the subject matter or materials discussed in the manuscript apart from those disclosed.

Address for correspondence:

Antonio Berruezo, MD, PhD

Heart Institute, Teknon Medical Center

C/ Vilana, 12; 08022 Barcelona (Spain)

Phone: +34 932 90 62 00 / Fax: +34 932 11 26 90

Email: antonio.berruezo@quironsalud.es

Word count: 3660

INTRODUCTION

Substrate-based catheter ablation is an effective, invasive treatment for recurrent episodes of scar-related ventricular tachycardias (VT), but the rate of recurrences remains still high. (1) Analyzing all the intracardiac electrograms requires acquiring a full electroanatomical map (EAM) of the area of interest, a process which is challenging and time-consuming. This increases the likelihood of having procedure-related complications.

One of the main objectives of VT substrate ablation procedures is to localize and ablate the site of origin (SOO, exit site) of the clinical VT, whose localization can be inferred from the VT morphology in the 12-lead ECG. (2) There are several algorithms that help localizing the SOO from ECG tracings, but they are solely based on visual inspection on the ECG, use nonstandard definitions for heart regions/areas and/or have applicability restrictions that prevent their use in all myocardial substrates. (3)

On the other hand, VT substrate ablation requires eliminating not only the clinical VT-SOO, but the whole arrhythmia substrate to abolish additional VT circuits. (4–6) Recent studies have showed that guiding the ablation with color-coded pixel signal intensity (PSI) maps delivered from pre-procedural late gadolinium enhancement cardiac magnetic resonance (LGE-CMR) imaging, results in more efficient procedures and improved VT recurrence-free survival. (7–9)

We hypothesize that the identification of scar-related VT-SOO can be fully automated by combining the surface ECG and the LGE-CMR imaging data into a machine learning (ML) algorithm integrated into a commercially available post-processing software. This is a proof-of-concept study to evaluate the feasibility of the ML algorithm and usefulness of the new software.

METHODS

Study populations

Training population

To train the ML model, all patients with documented VTs in a 12-lead surface ECG who were referred for ablation from January 2015 until December 2019 were included in the study, irrespectively of the presence of structural heart disease (SHD). Patients with ventricular arrhythmias arising from the right ventricle were excluded.

Validation population

To test the ML model's accuracy, consecutive patients with scar-related (reentry mechanism) sustained VTs referred for ablation (i.e. invasive treatment of the arrhythmia) from December 2019 until July 2020 were included.

The study complied with the Declaration of Helsinki, and the local ethics committee approved the study protocol.

Study workflow and objectives

The first step of the study was to develop and evaluate a complete pipeline that uses the surface ECG for predicting the SOO/SgO (site/segment of origin) of scar-related VTs (figure 1). A total of four ML models were used to predict/classify the location of the VT-SgO from the VT-ECG tracings, using the *American Heart Association* (AHA) 17-segment model.

The second step was to integrate this pipeline into current commercial software (ADAS 3D LV, ADAS3D Medical SL, Barcelona, Spain). This commercial software, with CE- and FDA-approval, identifies, from pre-procedural LGE-CMR imaging data, the border zone corridors (BZC) embedded within the myocardial scar structure. It also allows to export the PSI maps to the EAM navigation systems to guide ablation procedures.

The new version of the software is intended to predict the VT-SgO using multimodal, non-

invasive information: from pre-procedural 12-lead ECG and LGE-CMR. The primary objective of the study is to test the complete integration of the new software into the clinical practice, evaluating its accuracy in a prospective series of patients referred for VT substrate ablation.

Reference algorithm for VT-SOO/SgO detection

A previously described visual ECG algorithm (3) was used as a reference to compare the sensitivity and specificity of the algorithm trained by ML with real anatomical reference. This visual algorithm can be used to predict the SgO of LV scar-related VT regardless of the underlying heart disease and the epicardial versus endocardial VT origin. Briefly, the method is based on QRS axis in the frontal plane and transition in V3/V4 precordial leads (figure 2); the SgO is referred using the AHA 17-segment model. (10)

Development of machine learning models for VT-SOO/SgO detection

The development of the model consists in an annotation phase and a training phase. The annotation phase consists in retrieving the data to be processed. The model training, on its behalf, consists of the following steps (figure 1): data selection and preprocessing, data augmentation, feature extraction, feature selection and model training.

Annotation phase

The data annotation phase was performed by extracting the VT-ECG morphologies and their respective associated SgO for the study population. For this purpose, both clinical VTs and paced QRS morphologies from the LV were included in the database. Clinical VTs were included whenever their SOO/SgO could be reliably identified from the EAM data during ablation procedures. For paced morphologies, the location of the catheter when stimulating was considered the SOO/SgO. The above identified locations in the EAM were subsequently projected into the PSI maps and were, in turn, used as classification targets for the identification

of the VT-SgO, by assigning the closest element in the AHA 17-segment model. In cases when the SOO occurred at the intersection of several segments, the most probable one was marked as valid and the remaining plausible segments were stored for further data augmentation. A secondary set of annotations, for completeness, was registered taking into account signal-based criteria for the identification of the SgO according to a clinical algorithm. (3) Once the SgO associated to the morphology was annotated, the QRS complex was manually delineated by a cardiac electrophysiologist, marking its onset and offset.

Training phase

- Data selection: The first step of the training phase is data selection, which consists in the division of the dataset into non-overlapping train and test sets, containing 50% of the data each, in a stratified manner. The training set was used for model development and tuning, whereas the test set was reserved for assessing the model's performance. Data preprocessing, whose focus is finding better data representations for increasing model robustness, was performed in two steps. Firstly, the QRS was manually delineated. Secondly, the selected QRS was cropped, zero-corrected, and scaled to the magnitude of the highest voltage lead within the beat. Data augmentation, on its behalf, consisted in the application of mix-up, an all-purpose data augmentation technique that creates synthetic datapoints from the existing database, allowing for a better identification of the inter- and intra-segment separation criteria.
- Feature extraction: The second step of the training phase was feature extraction, which was performed by retrieving a set of signal-based, wavelet-based and spectral-based features specifically tailored towards ECG processing. These features allow the description of the data to be analyzed in a more robust manner, by structuring the difficult-to-process raw ECG recording into a finite set values that have semantical meaning. These features comprise the computation of intra-lead (e.g. min/max

voltages/areas or aggregate of magnitudes of different frequential bands), inter-lead (e.g. does lead I have a higher magnitude than lead III?) and global (e.g. precordial transition location according to different means of computation) characteristics. A total of 357 markers of the QRS complex were extracted for characterizing its behavior.

- Model training: The extracted features were then employed for training a classification model, support vector machines (SVM). A forward feature selection step was also used to filter out features that were highly correlated or that did not enhance the model's accuracy. (11) The model was trained using 5-fold cross-validation for finding the most appropriate model configuration.

The model's performance was assessed by comparing the predicted and the true SgO on the held-out test set, and compared to its clinical counterpart. Given the probabilistic formulation of the model, a secondary measurement of performance was provided, consisting in the accumulated accuracy to the second and third most probable SgO within the prediction.

Anatomic reconstruction of the heart and scar characterization using LGE-CMR

The validation population consisted of 15 consecutive patients with scar-related (reentry mechanism) sustained VTs referred for ablation (i.e. invasive treatment of the arrhythmia). All of them underwent a LGE-CMR test prior the procedure using a 1.5-Tesla scanner (ACHIEVA, Philips Healthcare, Best, The Netherlands). Contrast-enhanced images were acquired 10 minutes after bolus injection of 0.2 mmol/Kg Gadobutrol (Gadoyist®, Bayer Hispania, Barcelona, Spain) using a commercially available, free-breathing, ECG-gated, navigator-gated, 3D inversion-recovery, gradient-echo technique. Slice thickness was 1.4 mm, with no gap between slices. The field of view was set at 360 mm and matrix size was kept to 256 x 256 pixels to yield an isotropic spatial resolution of 1.4 x 1.4 x 1.4 mm. In patients previously

implanted with an ICD, LGE-CMR was performed using a specific wideband sequence to avoid device artefacts.

All LGE-CMR images were analyzed using a previously described protocol. (12) A full left ventricular (LV) volume was reconstructed in the axial orientation, and the resulting images were processed with ADAS 3D LV software (ADAS3D Medical SL, Barcelona, Spain). Color-coded pixel signal intensity (PSI) maps based on LGE-CMR images were projected to 10 myocardial shells (from endo- to epicardium), following a trilinear interpolation algorithm. The hyperenhanced area was characterized as core zone, border zone (BZ) or healthy tissue using 40 ± 5% and 60 ± 5% of the maximum PSI as thresholds. (12) The total scar mass, BZ mass, and core mass in each shell were automatically measured using the ADAS 3D LV software. Scar heterogeneity was defined as BZ percentage of the scar. BZ channels (BZCs) were defined as continuous corridors of BZ surrounded by scar core or an anatomical barrier (i.e. mitral annulus) connecting two areas of healthy tissue. The BZC mass was automatically computed using a full-automated tool embedded within the ADAS 3D LV software.

Pipeline integration into ADAS 3D LV software

The· SVM classifier incorporated into the ADAS 3D LV software to enable identifying the location of the SgO from the VT-ECG tracings, using the American Heart Association (AHA) 17-segment model. The new analysis allowed to import and visualize the ECG-signals from several polygraphs and includes a new user interface to select the QRS of the VT. Once the QRS is selected, the software executes the SVM for that particular QRS to obtain the SgO. Then, the probability of each AHA segment of being the VT-SgO was visualized in a table (figure 3). The software also includes a new visualization method to display the calculated SgO overlaid onto the LV visualization of the patient. This visualization allows the user to see together the post-infarction scar structure derived from the LGE-CMR and the VT-SgO

overlaid onto the LV. This further allows the user to even identify the heterogeneous tissue corridor that could be likely responsible for the reentry circuit causing the VT (figure 4). Finally, the user can export the results to the EAM navigation system in order to guide ablation procedures.

Prospective validation during VT ablation procedures

Unselected patients with documented scar-related VT, who were referred for VT substrate ablation, were consecutively enrolled to test the new ML-trained model of VT-SgO detection. The ablation procedures were performed according to a previously described protocol. (8) Briefly, the first step of the procedures was the acquisition of a fast anatomical map of the aorta, which was then used to integrate the anatomical heart reconstructions derived from a multidetector cardiac tomography and the LGE-CMR within the spatial reference coordinates of the CARTO3 (Biosense Webster, Diamond Bar, CA, USA) electroanatomic navigation system. The actual SgO of each VT was identified according to either one of the following criteria: i) Presence of presystolic local electrograms not earlier than 50 ms before the beginning of the QRS and termination of the VT during RF ablation or slow conducting channel exit site confirmed through entrainment maneuvers together with VT termination during RF ablation; or ii) achieving a 12/12 QRS morphology concordance with the 12-lead ECG of the VT during pacing from a site with no more than 50 ms delay between the stimulus artifact and the beginning of the QRS. The selection of the pacing sites was primarily based on the presence of BZC entrances identified by the pre-procedural CMR. Based in previous clinical experience, there is usually about one BZC entrance per AHA segment; that is, the identification of a VT-SgO usually identifies the BZC likely responsible of being the ‘critical isthmus’ of the VT reentry circuit (figure 5).

In order to test the accuracy of the new software for VT-SgO identification, once the actual SgO was recognized, it was compared with the SgO proposed by the software and the SgO predicted by the reference visual algorithm. The actual VT-SgO was identified according to data derived from the ablation procedures, anatomically referenced using either one of the following imaging datasets integrated during the interventions: electroanatomical maps, cardiac tomography, or LGE-CMR. Finally, a descriptive analysis of the presence of CMR-derived BZC at the predicted VT-SgO was performed, to estimate the potential ability of the software to predict the effective ablation target site. (8,13)

Statistical analysis

Continuous variables are given as mean ± standard deviation or median (interquartile range), as appropriate. Confidence intervals (CI, $\alpha = 0.05$) are provided for the model's performance metrics. Categorical variables are given as total number and percentages. To compare the means of 2 variables, the Student t-test or Wilcoxon test were used, as appropriate. Proportions were compared using the χ_2 or Fisher exact test, as appropriate. $P < 0.05$ was considered of statistical significance. Statistical analysis was performed using IBM SPSS Statistics, version 26.0 (IBM Corp. Released 2019; Armonk, NY: IBM Corp.).

RESULTS

Study populations

For the training phase of the ML algorithm, a total of 209 VT morphologies corresponding to 104 patients, recruited from 2015 until December 2019, were used. For the pilot validation of the ML model, 15 additional patients ('validation population') were prospectively recruited from January until July 2020. The baseline characteristics of these populations are shown in table 1. In the validation population, 15 clinical VT morphologies were analyzed with the ML model embedded in the ADAS software platform. Additionally, 62 non-clinical VT morphologies were induced by pacing the LV at different sites during the ablation procedures, locating the tip of the catheter at different BZC entrances previously identified with the LGE-CMR. Therefore, a total of 77 potential VT morphologies were used for final testing.

ML model performance

In the training phase (209 VT morphologies), the ML model provided a one-segment accuracy of 77%, ($CI_{95\%}$ 71 – 83%) with respect to the real signal-based SgO, whereas if the second most probable SgO was considered its accuracy raised to 92% ($CI_{95\%}$ 88 – 95%), and to 94% ($CI_{95\%}$ 90 – 97%) if the third most probable SgO was given as valid. The reference visual algorithm reached a score of 81%, ($CI_{95\%}$ 72 – 89%) on the same dataset. The reference algorithm performed similarly when compared to the one-segment prediction of the ML model ($p = 0.32$), but worse if taking as valid the best two or three SgO proposed by the model ($p = 0.001$ and $p = 0.0001$, respectively).

For the validation population (77 VT morphologies), the ML provided a one-segment accuracy of 88% ($CI_{95\%}$ 79 – 95%), 99% ($CI_{95\%}$ 93 – 100%) when considering the second most probable VT-SgO, and 100% ($CI_{95\%}$ 95 – 100%) when considering the third most probable VT-SgO. The reference visual algorithm reached a score of 91%, ($CI_{95\%}$ 82 – 96%) on the same dataset. The

reference algorithm performed similarly when compared to the one-segment prediction of the ML model ($p = 0.55$), but worse if taking as valid the best two or three SgO proposed by the model ($p = 0.005$ and $p = 0.002$, respectively). Figure 6 shows an example of correlation between the VT-SgO predicted by the reference visual algorithm (operator-dependent) and the ML model, integrated with the LGE-CMR information and ready to be used with the ADAS 3D LV customized software.

Correlation between scar characteristics and predicted VT-SgO

Main ablation results of the validation population are shown in table 2. All the patients had an inducible clinical VT; additionally, a mean of 4.1 ± 0.4 potential VT morphologies per patient were simulated by pacing the LV at different CMR-derived BZC entrances (figure 5). The identified myocardial scars (n = 15) occupied an area encompassing a median of 5 (4 – 6) AHA segments, thus representing a total of 74/255 (29%) scarred AHA segments. A total of 68 BZC entrances were identified, thus representing a median of 0.83 (0.8 – 1) BZC entrances per scarred segment. There were only 2/74 (3%) AHA segments showing more than one BZC entrance; one of them corresponded to a clinical VT-SgO, the other one to a paced VT morphology.

DISCUSSION

The main findings of the study are:

- This is the first clinical study to show the feasibility of training and integrating a ML model of non-invasive surface ECG data into the pipeline of a commercially available software (ADAS 3D LV) that allows to correlate ECG and anatomy by characterizing the myocardial scar from LGE-CMR studies. The clinical relevance comes from the fact that this pipeline may allow to standardize the invasive treatment (ablation) in patients that have suffered from life-threating VTs.
- This study proves additional advantages of the use of ML when interpreting ECG tracings. When compared to a reference visual model, based on operator's expertise, (3) it shows a similar accuracy in terms of best predicted SgO, but it can further identify more SgO by suggesting up to 3 adjacent –and potential– SgO.
- There was a median of 0.83 (0.8 – 1) CMR-derived BZC entrances per scarred segment. These are considered ablation targets for invasive treatment of scar-related reentrant VTs. (8,13) Thus, the automatic identification of the VT-SgO using the proposed usable software-based pipeline almost equals the identification of the putative BZC being the critical isthmus of the reentry VT circuit.

With regards to the first and second points, the developed ML model has many advantages for the prediction of the VT-SgO location. On the first hand, it is flexible, facilitating the identification of non-linear relationships between the input data. Secondly, a probabilistic formulation is available, allowing for stratifying the prediction by returning a hierarchy of probabilities of adherence to a specific AHA segment instead of a single value. Reentrant VTs exit sites, which correspond to BZC entrances identifiable after post-processing a LGE-CMR, are not always found 'at the center' of a given AHA segment. On the contrary, BZC entrances can be found at any point of the LV anatomy, and, therefore, it is not uncommon to find them

close to the hypothetical boundary between 2 segments, or even more than 2. These localization differences represent mm or few cm of distance, but they can determine subtle changes in the morphological characteristics of the ECG. These distinctions may be incorporated when training a ML model, but they seem difficult to be merged into visual algorithms reliant on operator's knowledge.

The identification of the VT-SgO seems useful, since at this anatomical level it is possible to find at least one BZC entrance. BZC are, as already defined, corridors of heterogeneous (viable) myocardial tissue surrounded by dense scar and connecting two areas of healthy myocardium. It is an anatomical concept, based on what can be revealed when performing an LGE-CMR. This imaging technique is recognized as the gold standard to determine the location and extent of myocardial scar. (14) There is proven correlation between the anatomical findings of the CMR and functional electrophysiology: the CMR-defined scar has a good correlation with low-voltage areas in the electroanatomical maps (EAM), (15,16) and the presence of BZC is related to the presence of slow conducting channels within the scar. (15,17) Moreover, the size and heterogeneity of the post-MI scar, as evaluated with CMR, are variables that have been associated with VT inducibility, (18,19) arrhythmia events, and even mortality. (20–22)

Ventricular tachycardia (VT) substrate ablation is an effective treatment for patients that suffer from recurrent episodes of scar-dependent VTs. (23,24) However, different substrate-guided approaches have been proposed; targeting conducting channels based on timing of delayed electrogram components during sinus rhythm (scar dechanneling) has proven to be an effective approach. (6,13) Recently, CMR-guided VT ablation based on scar dechanneling has proven to halve the time required for the procedure, significantly reducing the need of fluoroscopy and radiofrequency delivery, and being associated with a a higher ventricular arrhythmia-free survival. (8)

All the aforementioned, the ability to automatically localize the BZC (and its entrance) from ECG and CMR data would permit to standardize ablation procedures, to shorten the time from the insertion of the catheter until abolition of the documented VT and, likely, to improve safety and reliability of these procedures.

Study limitations

An important limitation is the necessity of the actual pipeline to rely on manual identification of the QRS segment. The existing tools for delineation are often faced with poor performance on complex rhythms such as VT. The development of all-purpose, robust tools for wave delineation can fully automatize the developed pipeline. Finally, classical ML approaches are overtly reliant on the extraction of quality features for describing the data to be analyzed. More detailed spectral-, signal- or wavelet-based features could be applied for more adequate data representation.

Future directions

- The ability to import ECG tracings not only from specific electrophysiology recording systems in the cath lab, but also from ambulatory digital ECG recorders, or even paper (analogical) tracings would be a milestone on the path towards clinical applicability. Patients suffering from life-threating VTs would have an ECG from the emergency department; this ECG could be automatically imported into ADAS 3D LV, and analyzed together with the LGE-CMR to plan the invasive treatment and select the best ablation target, all in a full automated way.
- Other ML approaches, such as directly using raw ECG data with deep learning algorithms, could also be explored. Deep learning typically yields an increased

performance, although these models require larger amounts of annotated data, besides producing black-box models that are difficult to interpret. (25)

- Some methodologies based on deep learning have shown promising results for automatic ECG delineation. Although the database employed for developing models for automatic ECG delineation do not perform adequately on complex morphologies such as sustained ventricular tachycardias, recent developments in the machine learning field could allow extending currently developed models to adapt to VT morphologies, enabling fully automated SgO identification.

Conclusions

The identification of scar-related VT-SgO and the putative BZC responsible for the reentry VT circuit can be fully automated by combining the surface ECG and the LGE-CMR imaging data into a machine learning (ML) algorithm integrated into a commercially available post-processing software. This could allow for standardization of ablation (i.e. treatment) interventions for these life-threatening arrhythmias.

ACKNOWLEDGEMENTS

None.

FUNDING

This research received a grant from the ATTRACT Project, part of the European Union's Horizon 2020 research and innovation program (grant agreement No. 777222).

REFERENCES

1. Tilz RR., Eitel C., Lyan E., et al. Preventive ventricular tachycardia ablation in patients with ischaemic cardiomyopathy: Meta-analysis of randomised trials. Arrhythmia Electrophysiol Rev 2019. Doi: 10.15420/aer.2019.31.3.
2. Yokokawa M., Liu TY., Yoshida K., et al. Automated analysis of the 12-lead electrocardiogram to identify the exit site of postinfarction ventricular tachycardia. Hear Rhythm 2012. Doi: 10.1016/j.hrthm.2011.10.014.
3. Andreu D., Fernández-Armenta J., Acosta J., et al. A QRS axis–based algorithm to identify the origin of scar-related ventricular tachycardia in the 17-segment American Heart Association model. Hear Rhythm 2018. Doi: 10.1016/j.hrthm.2018.06.013.
4. Jaïs P., Maury P., Khairy P., et al. Elimination of local abnormal ventricular activities : A new end point for substrate modification in patients with scar-related ventricular tachycardia. Circulation 2012. Doi: 10.1161/CIRCULATIONAHA.111.043216.
5. Di Biase L., Burkhardt JD., Lakkireddy D., et al. Ablation of Stable VTs Versus Substrate Ablation in Ischemic Cardiomyopathy the VISTA Randomized Multicenter Trial. J Am Coll Cardiol 2015. Doi: 10.1016/j.jacc.2015.10.026.
6. Scar dechanneling: a new method for scar-related left ventricular tachycardia substrate ablation. Circ Arrhythmia Electrophysiol 2015.
7. Andreu D., Penela D., Acosta J., et al. Cardiac magnetic resonance–aided scar dechanneling: Influence on acute and long-term outcomes. Hear Rhythm 2017. Doi: 10.1016/j.hrthm.2017.05.018.
8. Soto-Iglesias D., Penela D., Jáuregui B., et al. Cardiac Magnetic Resonance−Guided Ventricular Tachycardia Substrate Ablation. JACC Clin Electrophysiol 2020;(December). Doi: 10.1016/j.jacep.2019.11.004.
9. Zghaib T., Ipek EG., Hansford R., et al. Standard Ablation Versus Magnetic Resonance

Imaging-Guided Ablation in the Treatment of Ventricular Tachycardia. Circ Arrhythmia Electrophysiol 2018. Doi: 10.1161/CIRCEP.117.005973.

10. Cerqueira MD., Weissman NJ., Dilsizian V., et al. Standardized myocardial sementation and nomenclature for tomographic imaging of the heart: A Statement for Healthcare Professionals from the Cardiac Imaging Committee of the Council on Clinical Cardiology of the American Heart Association. Circulation 2002. Doi: 10.1161/hc0402.102975.

11. Chandrashekar G., Sahin F. A survey on feature selection methods. Comput Electr Eng 2014. Doi: 10.1016/j.compeleceng.2013.11.024.

12. Andreu D., Ortiz-Pérez JT., Fernández-Armenta J., et al. 3D delayed-enhanced magnetic resonance sequences improve conducting channel delineation prior to ventricular tachycardia ablation. Europace 2015. Doi: 10.1093/europace/euu310.

13. Berruezo A., Fernández-Armenta J., Andreu D., et al. Scar dechanneling. Circ Arrhythmia Electrophysiol 2015. Doi: 10.1161/CIRCEP.114.002386.

14. Cronin EM., Bogun FM., Maury P., et al. 2019 HRS/EHRA/APHRS/LAHRS expert consensus statement on catheter ablation of ventricular arrhythmias. Hear Rhythm 2020. Doi: 10.1016/j.hrthm.2019.03.002.

15. Fernández-Armenta J., Berruezo A., Andreu D., et al. Three-dimensional architecture of scar and conducting channels based on high resolution ce-CMR: Insights for ventricular tachycardia ablation. Circ Arrhythmia Electrophysiol 2013. Doi: 10.1161/CIRCEP.113.000264.

16. Gupta S., Desjardins B., Baman T., et al. Delayed-enhanced MR scar imaging and intraprocedural registration into an electroanatomical mapping system in post-infarction patients. JACC Cardiovasc Imaging 2012. Doi: 10.1016/j.jcmg.2011.08.021.

17. Perez-David E., Arenal Á., Rubio-Guivernau JL., et al. Noninvasive identification of

ventricular tachycardia-related conducting channels using contrast-enhanced magnetic resonance imaging in patients with chronic myocardial infarction: Comparison of signal intensity scar mapping and endocardial voltage mappin. J Am Coll Cardiol 2011. Doi: 10.1016/j.jacc.2010.07.043.

18. Bello D., Fieno DS., Kim RJ., et al. Infarct morphology identifies patients with substrate for sustained ventricular tachycardia. J Am Coll Cardiol 2005. Doi: 10.1016/j.jacc.2004.12.057.

19. Schmidt A., Azevedo CF., Cheng A., et al. Infarct tissue heterogeneity by magnetic resonance imaging identifies enhanced cardiac arrhythmia susceptibility in patients with left ventricular dysfunction. Circulation 2007. Doi: 10.1161/CIRCULATIONAHA.106.653568.

20. Yan AT., Shayne AJ., Brown KA., et al. Characterization of the peri-infarct zone by contrast-enhanced cardiac magnetic resonance imaging is a powerful predictor of post-myocardial infarction mortality. Circulation 2006. Doi: 10.1161/CIRCULATIONAHA.106.613414.

21. Klem I., Weinsaft JW., Bahnson TD., et al. Assessment of myocardial scarring improves risk stratification in patients evaluated for cardiac defibrillator implantation. J Am Coll Cardiol 2012. Doi: 10.1016/j.jacc.2012.02.070.

22. Ganesan AN., Gunton J., Nucifora G., McGavigan AD., Selvanayagam JB. Impact of Late Gadolinium Enhancement on mortality, sudden death and major adverse cardiovascular events in ischemic and nonischemic cardiomyopathy: A systematic review and meta-analysis. Int J Cardiol 2018. Doi: 10.1016/j.ijcard.2017.10.094.

23. Reddy VY., Reynolds MR., Neuzil P., et al. Prophylactic catheter ablation for the prevention of defibrillator therapy. N Engl J Med 2007. Doi: 10.1056/NEJMoa065457.

24. Kuck KH., Schaumann A., Eckardt L., et al. Catheter ablation of stable ventricular

tachycardia before defibrillator implantation in patients with coronary heart disease (VTACH): a multicentre randomised controlled trial. Lancet 2010. Doi: 10.1016/S0140-6736(09)61755-4.

25. Mincholé A., Camps J., Lyon A., Rodríguez B. Machine learning in the electrocardiogram. J Electrocardiol 2019. Doi: 10.1016/j.jelectrocard.2019.08.008.

TABLES

Table 1. Baseline characteristics of the ML training and validation populations. See text for details.

	Training population n = 104	**Validation population n = 15**	**p**
Age, y	68 ± 9	65 ± 12	0.25
Male, n (%)	85 (82)	13 (89)	0.50
HT, n (%)	74 (71)	11 (75)	0.75
DLP, n (%)	52 (50)	9 (63)	0.35
DM, n (%)	28 (27)	4 (27)	1.0
LVEF, %	37 ± 15	39 ± 18	0.64
LVEDD, mm	63 ± 8	61 ± 12	0.40
LVESD, mm	45 ± 13	43 ± 11	0.57
ICM, n (%)	85 (82)	13 (89)	0.50
Mean VT cycle length	323 ± 135	341 ± 143	0.63
ICD carriers before ablation [n (%)]	94 (90)	13 (89)	0.90
NYHA • **I, n (%)** • **II, n (%)** • **III, n (%)** • **IV, n (%)**	 29 (28) 60 (58) 15 (14) 0	 5 (34) 8 (54) 2 (14) 0	0.77
Approach • **Endo, n (%)** • **Endo/Epi, n (%)**	 76 (73) 28 (27)	 11 (75) 4 (25)	0.87
Indication • **Incessant VT, n (%)** • **Arrhythmic storm, n (%)**	 7 (7) 10 (10)	 2 (13) 1 (7)	0.42

***CMR**: cardiac magnetic resonance; **DLP**: dyslipidemia; **DM**: diabetes mellitus; **HT**: hypertension; **ICM**: ischemic cardiomyopathy; **LVEF**: left ventricle ejection fraction; **LVEDD**: left ventricle end-diastolic diameter; **LVESD**: left ventricle end-systolic diameter; **NYHA**: New York Heart Association functional class; **VT**: ventricular tachycardia.*

Table 2. Ablation results in the validation population (n = 15).

Procedure time (min)	103 ± 64
RF time (min)	12 ± 10
RF applications (n)	32 ± 23
Fluoroscopy time (min)	9 ± 5
Residual VT after substrate ablation, n (%)	5 (18)
Induced VT morphologies	1 (1 – 1)
Complications (%)	0
Final procedure success (n, %) • **Total** • **Partial** • **No**	 13 (87) 2 (13) 0 (0)

RF: *radiofrequency;* ***VT:*** *ventricular tachycardia.*

FIGURES

Figure 1. Employed machine learning (ML) pipeline. The first step consists in data annotation, where the onset and offset were annotated for the ECGs in the study population. The second step consists in data preprocessing, where the QRS' are isolated, normalized, divided into training/testing sets for ML model tuning, and augmented. The third step consists in the extraction of features for robust description of the input data; signal-based, wavelet-based and spectral-based features were extracted for all recordings in the train and test sets. The fourth step consists in model training from the extracted features in the training set. Finally, the fifth step evaluates the performance of the model in the features of the held-out test set.

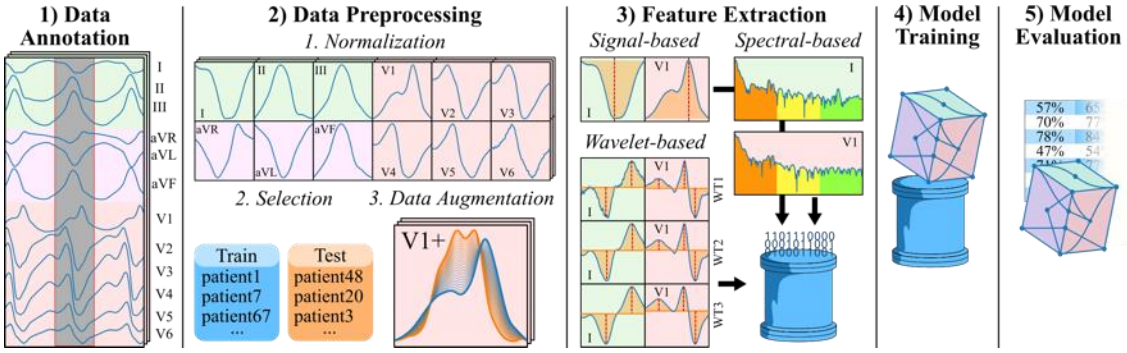

Figure 2. Example of application of the visual reference algorithm for identification of VT-SgO. Patient with ischemic cardiomyopathy and anteroapical transmural scar. The scar, visualized after CMR postprocessing using ADAS 3D LV (left panel), is characterized as core (dense fibrosis) in *red*, border zone (intermediate fibrosis, heterogeneous tissue) in *green*, and healthy myocardium in *pink*. The *red circle* marks the site of the clinical VT exit, which corresponds to a BZC entrance (*white line*). The 12-lead ECG of the VT is shown in the right panel. Regarding the VT morphology, the following considerations were made: Maximum absolute amplitude in ECG limbs: (+) III. Adjacent leads to (+) III: (+) aVF. Segment group considered: 1 / 7 / 13. Polarity in precordial leads: (-) V3 / (-) V4. Final Segment = 13 (apical anterior).

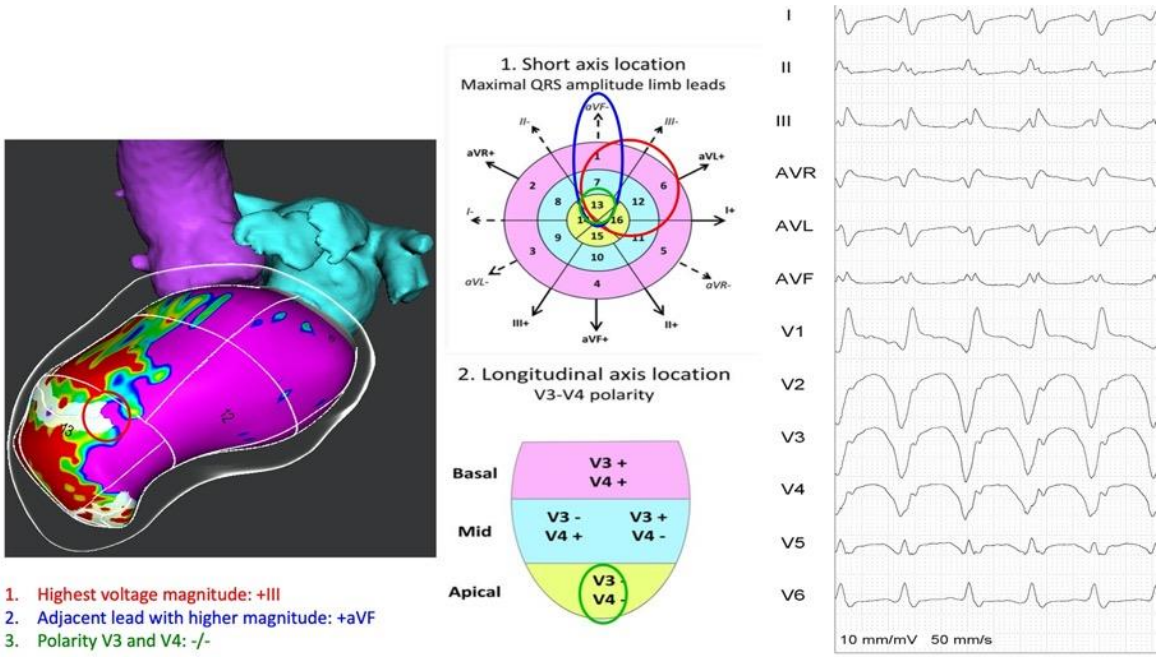

Figure 3. Example of the ADAS 3D LV interface showing a VT-ECG in a patient with an anteroseptal myocardial infarction. The manually selected start and end times of the QRS morphology are highlighted in the red box. After selecting the QRS, the SVM classifier is executed to calculate the VT-SgO. This calculates the probability of each AHA segment of being the VT-SgO. The software then displays the most probable segment (in this case, segment 2, or basal anteroseptal) and then the user can press the button 'Visualize Segment in 3D LV' which launches the screen of figure 4.

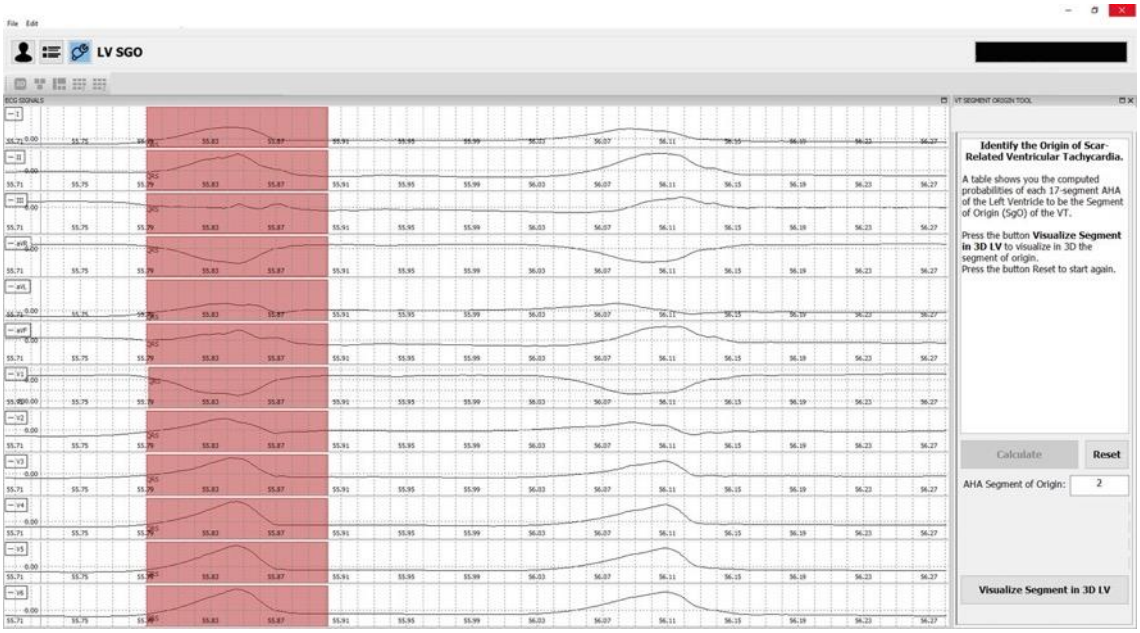

Figure 4. Predicted VT-SgO (AHA segment 2, or basal anteroseptal) in a patient with an anteroseptal myocardial infarction. The scar, visualized after CMR postprocessing using ADAS 3D LV, is characterized as core (dense fibrosis) in *red*, border zone (intermediate fibrosis, heterogeneous tissue) in *yellow*, and healthy myocardium in *blue*. The red lines surrounded by *white* represent the heterogeneous tissue corridors (border zone channels) embedded within the scar and calculated automatically. The AHA segment 2 is highlighted in yellow and indicates the exit of the putative responsible channel for the reentry circuit causing the VT. Ablation treatment could be then first directed to this area.

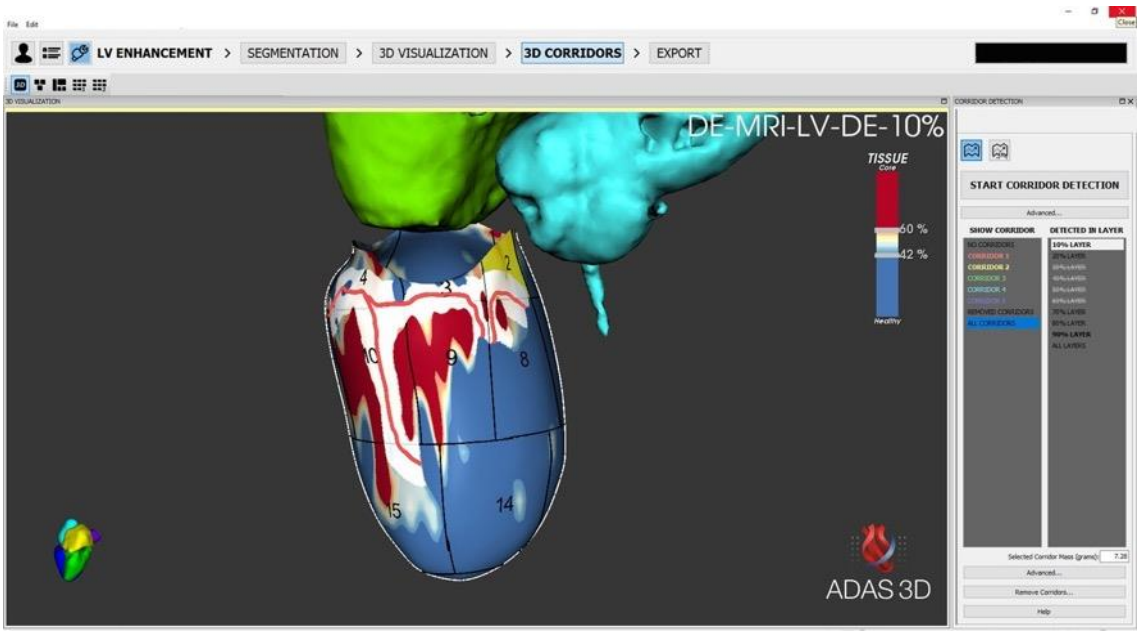

Figure 5. Predicted VT-SgO (AHA segment 9, or mid inferoseptal) in a patient with an inferior-inferoseptal myocardial infarction. The VT morphology was analyzed with the ADAS 3D LV software, which detected segment 9 as the most probable VT-SgO (segment 10 the second most probable). Using the same software, post-processing of the LGE-CMR to characterize the myocardial scar permitted to detect a BZC entrance just located in segment 9 (adjacent to segment 10). This BZC was considered responsible for the VT reentry circuit; its entrance acting as the 'exit site' during VT. Radiofrequency ablation of this BZC entrance rendered the VT non-inducible anymore.

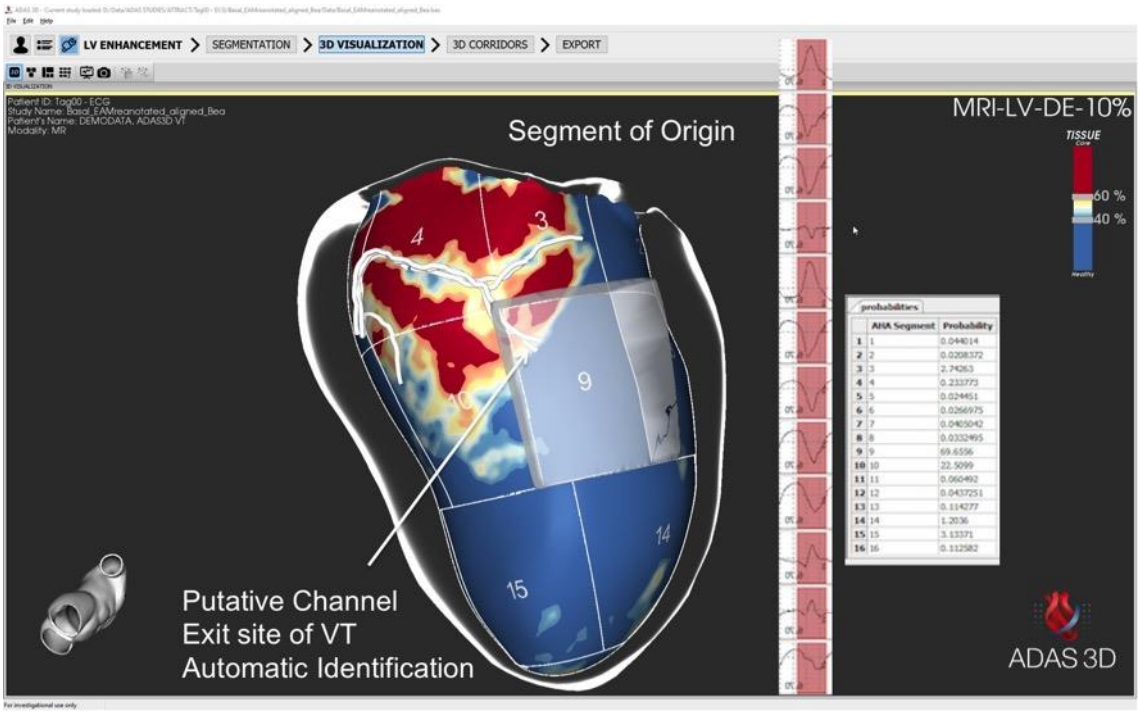

Figure 6. Prediction of the VT-SgO using the reference algorithm (visual) versus a complete automatic pipeline (ADAS 3D LV software with an integrated ML model to predict the VT-SgO plus scar characterization from LGE-CMR data). Patient with an inferolateral myocardial infarction referred for VT ablation. The VT morphology is shown (*black panel*). The reference algorithm (*left panel*) allows to predict segment 11 as the VT-SgO, but it requires a high level of knowledge in recognizing ECG tracings. The proposed pipeline using the new embedded tools in ADAS 3D LV software allows to predict the same SgO in an automatic way, besides recognizing the BZC responsible for the VT circuit and its entrance at the target SgO.